https://doi.org/10.5194/essd-2026-423
Preprint. Discussion started: 13 July 2026

Open Access Earth System Science Data Discussions

Physical and Geochemical Characterization of Mineral Dust Samples Collected by the DUST^2 Project and Precursors, 2011-2025

Jeffrey S. Munroe[1] and Diego P. Fernandez[2]

[1]Institute of Geology, University of Innsbruck, Innsbruck 6020, Austria
[2]Department of Geology & Geophysics, University of Utah, Salt Lake City, Utah, 84112, United States of America

Correspondence to: Jeffrey S. Munroe (Jeffrey.Munroe@uibk.ac.at)

Abstract

Mineral dust is a key component of Earth's Critical Zone, transporting minerals, nutrients, and trace elements across regions and linking distant components of the lithosphere, atmosphere, hydrosphere, and biosphere, yet quantitative understanding of these connections is limited by the availability of spatially distributed, well-characterized datasets. Here, we present a multi-year dataset of mineral dust samples collected as part of the DUST^2 Critical Zone Thematic Cluster and precursor projects using a network of 20 passive dust collectors deployed across a source-to-sink transect from arid dust-emitting regions of the Great Basin to downwind mountain environments in Utah, Nevada, and Idaho. The dataset includes measurements of major and trace element concentrations, CIELAB colour parameters, and grain size distributions, together with metadata describing sampling protocols, site characteristics, temporal coverage, and analytical methods. Consistent sampling and analytical procedures enable direct comparison across sites and years, supporting evaluation of spatial patterns in dust properties, and temporal variability associated with hydroclimatic forcing and land-surface change. This dataset is designed to support a wide range of applications, including dust source apportionment, evaluation of atmospheric transport and deposition models, and assessment of atmospheric contributions to soil development, nutrient cycling, and water quality in downwind ecosystems. By providing a standardized, openly accessible record of dust composition across a well-constrained source-to-sink system, this contribution enhances data availability for studies of aeolian processes and Critical Zone dynamics and provides a transferable framework for investigating dust-driven connectivity in other regions experiencing expanding dust emissions.

1 Introduction

Entrainment, transport, and deposition of mineral dust links the lithosphere, atmosphere, hydrosphere, and biosphere across a wide range of spatial and temporal scales (Shao et al., 2011). Dust carries a complex mixture of minerals, nutrients, and trace elements derived from both natural and anthropogenic sources, and its deposition influences soil formation (Munroe et al., 2024), air and water quality (Checketts et al., 2020), hydrology (Lang et al., 2026), ecosystems (Munroe et al., 2025; Nielson and Brahney, 2025), and society (Barnick et al., 2022) in downwind environments, making the dust cycle a key component of Earth's Critical Zone (Brahney et al., 2024; Munroe, 2026c). Despite its importance however, understanding of dust source-

https://doi.org/10.5194/essd-2026-423
Preprint. Discussion started: 13 July 2026

to-sink dynamics is complicated by the scarcity of well-characterized, spatially distributed datasets that capture both the composition and variability of deposited eolian material.

Geochemical characterization of mineral dust provides a critical foundation for investigation of the past and present dust cycle. Abundances of major and trace elements have been widely used to constrain dust provenance, quantify mixing among source regions, and evaluate the contribution of atmospheric inputs to soils and aquatic systems (Formenti et al., 2011, 2014; Rodríguez et al., 2011). However, existing datasets are often restricted in spatial extent or duration, limiting their applicability for regional synthesis or for integration with atmospheric transport models and ecosystem studies.

Here, we present a dataset of geochemical measurements from contemporary mineral dust samples collected with a network of passive dust collectors primarily deployed on mountain summits and high ridgelines in Utah, Nevada, and Idaho in the southwestern United States. Accompanying metadata document the collector design, sampling protocols, site characteristics, temporal coverage, and analytical methods, enabling reproducibility and facilitating integration with complementary datasets, including atmospheric modelling outputs, remote sensing products, and hydrological and ecological observations.

This contribution is intended to support a range of applications within Earth system science. These include (i) constraining dust provenance and quantifying source contributions using geochemical tracers, (ii) evaluating temporal variability in dust composition in response to climatic forcing and land-use change, (iii) informing atmospheric transport and deposition models, and (iv) assessing the role of dust as a vector for nutrients and contaminants in terrestrial and aquatic ecosystems. By providing a spatially extensive, multi-parameter dataset with consistent sampling and analytical protocols, this work contributes to ongoing efforts to improve data availability and interoperability for studies of aeolian processes and Critical Zone dynamics.

2. The Dust Collector Network

Beginning in 2011, a network of passive dust collectors was established to collect modern mineral dust arriving in mountain environments in the Intermountain West of the United States, the broad region between the Sierra Nevada and the Rocky Mountains. The design of the collectors (Fig. 1) was based on the marble dust trap typically used in dryland research, modified fur use in harsh, high-altitude environments with considerable snowfall (e.g. Reheis and Kihl, 1995; Wesely and Hicks, 2000; Sow *et al.*, 2006). Collectors are a clear polycarbonate tray measuring 56 x 56 cm by 7.5 cm deep divided into five “V-shaped” troughs, each of which is filled with ~400, 1.75-cm diameter glass beads (~7 kg per collector). The beads form a rough surface that traps dust from the air, protects previously deposited dust from the wind, and reduces the possibility of dust splashing out during precipitation events. The troughs inevitably collect water as well as dust, but the black beads heat in the sun to evaporate water between precipitation events. If the troughs completely fill, a row of small (3 mm) holes allows water to trickle out. Dust trapped by the beads settles to the base of each trough where it remains as water evaporates. Technical build sheets

https://doi.org/10.5194/essd-2026-423
Preprint. Discussion started: 13 July 2026

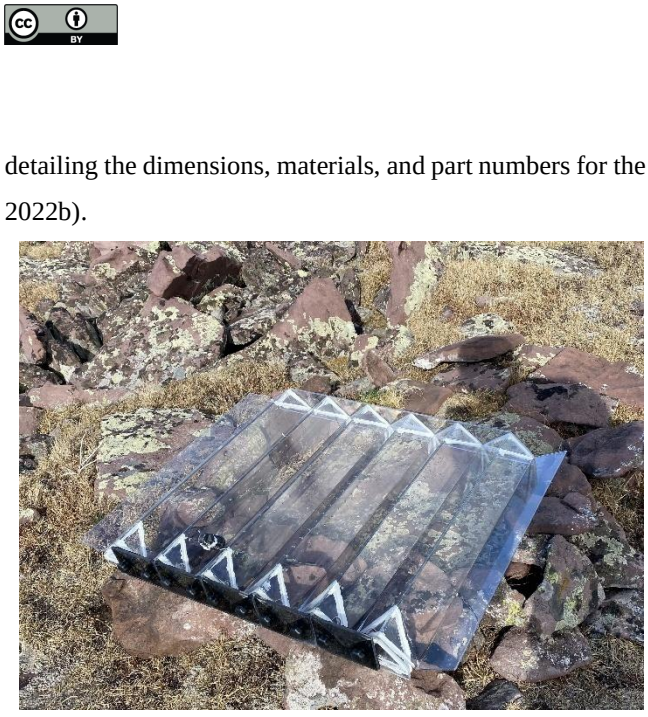


Figure 1. Photographs of dust collectors showing their design and typical deployments. Upper left: the DUST-7 collector in position before the glass beads were added. Upper right: the DUST-2 collector deployed in the Uinta Mountains. The collector was intentionally located in this periglacial rockfield to reduce the potential for locally sourced soil particles to saltate into the collector, contaminating the exotic dust. Lower left: the DUST-11 collector in the Ruby Mountains of Nevada. The collector was surrounded by a low wall of rocks to protect it from winter winds in this exposed location. Lower right: the DUST-3 collector in the Uinta Mountains. Again, the location was selected to reduce the potential for contamination by local soil, and the collector is stabilized by a surrounding wall of rocks.

Initially the collector network (Fig. 2) focused solely on the Uinta Mountains in northeastern Utah, a setting where previous work had noted a ubiquitous layer of fine silt capping soil profiles that was interpreted as an alpine loess deposit, as well as the presence of abundant clay minerals in alpine soils, which was unexpected given the weathering-resistant quartzite bedrock (Bockheim et al., 2000; Bockheim and Koerner, 1997). The first four collectors were deployed as proof of concept, yielding insights into the flux and composition of modern dust in these mountains (Munroe, 2014; Munroe et al., 2015). Four more collectors were added in 2015 as part of a project funded by the US National Science Foundation "*Alpine Loess, Periglacial*

https://doi.org/10.5194/essd-2026-423
Preprint. Discussion started: 13 July 2026

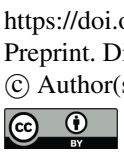

Open Access Earth System Science Data Discussions

Uplands, and Exotic Additions: Investigating Past and Present Dust Deposition in the Alpine Zone of the Uinta Mountains, Utah." This more comprehensive network supported identification of likely dust sources (Munroe et al., 2019), quantification of the dust component of alpine soils (Munroe et al., 2020), and reconstruction of dust flux variations through the Holocene (Munroe et al., 2021). The collector network was expanded further starting in 2020 at the start of the *DUST^2 (Dust across a Desert-Urban-Summit Transect)* project, a component of the Critical Zone Collaborative Network, also supported by the US National Science Foundation. In addition to the established collectors in the Uinta Mountains, the DUST^2 network included collectors at lower elevations in the cities of Salt Lake City and Provo, Utah, which helped disentangle mixing of natural and anthropogenic dust (Munroe et al., 2025), as well as collectors on mountain summits and high ridgelines in southern Utah, Nevada, and Idaho, which helped further constrain dust provenance and impacts on alpine soil development (Munroe et al., 2023, 2024). The final network consisted of 20 collectors (DUST-1 through DUST-20), the oldest four of which (DUST-1 through DUST-4) were deployed continually from 2011 through 2025 (Fig. 2, Table 1).

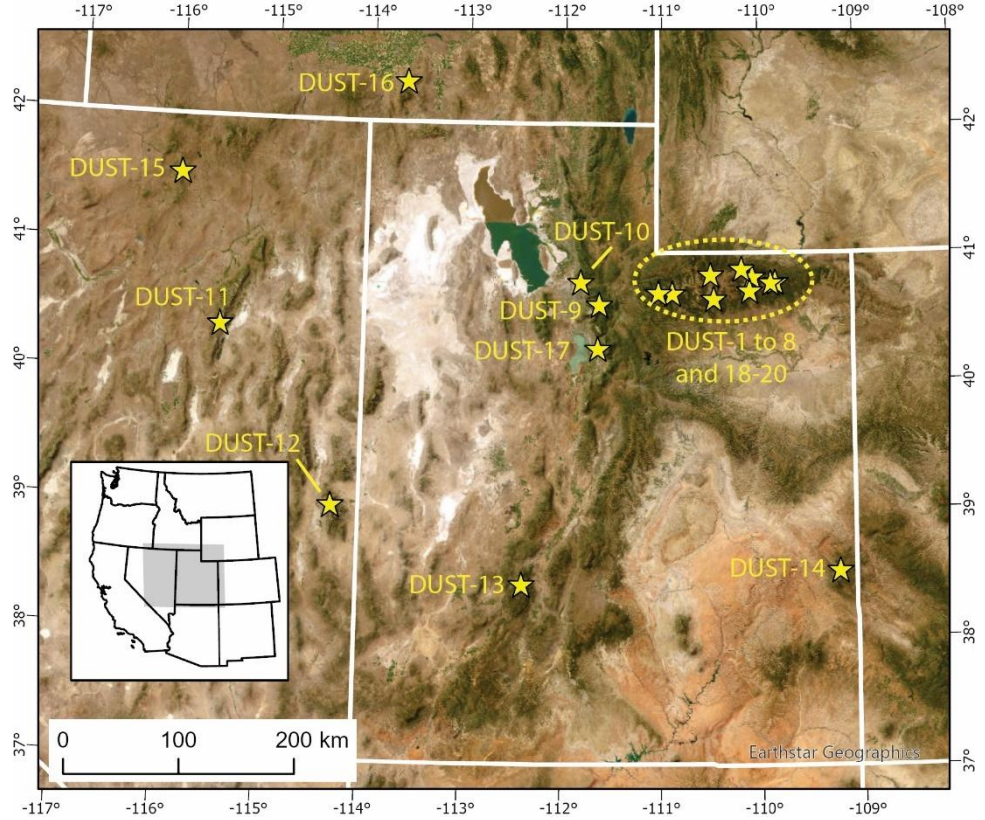

Figure 2. Locations of the 20 passive dust collectors (yellow stars). The oval surrounds DUST-1 through DUST-8, and DUST-18 through DUST-20 in the Uinta Mountains of northeastern Utah. Background is a true-colour satellite image from Earthstar Geographics © 2023 (World Imagery – Overview, 2023). Inset shows the location of the larger map (grey box) within the western United States.

https://doi.org/10.5194/essd-2026-423
Preprint. Discussion started: 13 July 2026

Open Access Earth System Science Data Discussions

Table 1: Locations of Dust Collectors

Collector	*Latitude d.ddddd*	*Longitude d.ddddd*	*Elevation m*	*Location --*	*State --*	*Deployed --*
DUST-1	40.80997	-110.07345	3692	Uinta Mountains	Utah	6/29/2011
DUST-2	40.63857	-110.46599	3410	Uinta Mountains	Utah	6/30/2011
DUST-3	40.68024	-110.88894	3396	Uinta Mountains	Utah	7/1/2011
DUST-4	40.82628	-110.49868	3795	Uinta Mountains	Utah	7/2/2011
DUST-5	40.70105	-110.10081	3592	Uinta Mountains	Utah	10/2/2015
DUST-6	40.68420	-111.02984	3413	Uinta Mountains	Utah	10/4/2015
DUST-7	40.87069	-110.18256	3589	Uinta Mountains	Utah	10/5/2015
DUST-8	40.76839	-109.83412	3667	Uinta Mountains	Utah	10/6/2015
DUST-9	40.59126	-111.63770	2671	Wasatch Mountains	Utah	9/17/2020
DUST-10	40.76668	-111.82842	1520	Salt Lake City	Utah	11/25/2020
DUST-11	40.37586	-115.50140	2881	Ruby Mountains	Nevada	9/19/2020
DUST-12	38.99199	-114.31727	3684	South Snake Range	Nevada	9/21/2020
DUST-13	38.40102	-112.39293	3456	Tushar Mountains	Utah	9/23/2020
DUST-14	38.51652	-109.21864	3669	La Sal Mountains	Utah	9/24/2020
DUST-15	41.54140	-115.96658	3021	Independence Range	Nevada	6/26/2021
DUST-16	42.31171	-113.65120	2785	Albion Range	Idaho	7/4/2021
DUST-17	40.24719	-111.65015	1422	Provo	Utah	7/20/2021
DUST-18	40.57395	-111.04351	2391	Uinta Mountains	Utah	10/11/2021
DUST-19	40.76468	-109.88189	3518	Uinta Mountains	Utah	10/8/2022
DUST-20	40.76435	-109.88274	3537	Uinta Mountains	Utah	10/8/2022

3. Methods

3.1 Field Methods

The elegance of a passive dust collector is its simplicity. There are no moving parts to fail, no power source that needs to be maintained, and no delicate components that could be damaged by harsh conditions. This same goal of simplicity carried over to the equipment used to remove the dust from a collector. Everything needed for field servicing was intended to be simple, robust, and easy to replace if necessary. Accordingly, only the following items were needed:

- Five, 1-L low density polyethylene bottles (Nalgene) full of distilled water (washed with 3% trace metal grade HNO_3 before use)
- Another empty 1-L Nalgene bottle (also acid-washed)
- A large plastic slotted spoon
- A colander
- A large plastic funnel
- A toothbrush
- A turkey baster

https://doi.org/10.5194/essd-2026-423
Preprint. Discussion started: 13 July 2026

- Five plastic bags (Ziplock)

These simple items were utilized in a consistent procedure to remove the dust from the collectors (Fig. 3). First, a small amount of water (<100 ml) was poured over the glass beads in a given trough to wet the collected dust so that it could not be blown away after the protective layer of beads was removed. The beads were then scooped from the trough with a clean slotted spoon, and transferred to a colander (Fig. 3). The colander was placed in the funnel, which was centred in an acid-washed Nalgene bottle. The beads in the colander were washed with ~500 ml of distilled water, stirred with the spoon, and washed again with an additional ~500 ml of distilled water. The beads were then transferred to a clean 4 L plastic bag, and the baster was used to suck up any water that had been added to secure the dust, plus any water remaining from recent precipitation (Fig. 3). This water was added to that in the Nalgene bottle, and the bottle was capped. This process was repeated for the other four troughs so that all the beads were distributed into 5 plastic bags, and five Nalgene bottles were filled with water containing the material washed from the beads.

https://doi.org/10.5194/essd-2026-423
Preprint. Discussion started: 13 July 2026

Figure 3. Photographs of the dust collectors and the process of emptying them. Upper left: scooping the black glass beads from the DUST-11 collector into a colander for rinsing. Upper right: using the baster to suck up water and dust from the troughs of the DUST-7 collector after removing and washing the glass beads. Lower left: tilting the collector and removing the gasketed door from the end of one trough. Lower right: five 1 L bottles of dirty distilled water containing the dust washed from the DUST-16 collector.

Next, a gasketed cap secured with two thumb-screws was removed from the end of a trough, and the entire collector was tilted toward the open end that was positioned over the funnel again centred in an empty Nalgene bottle (Fig. 3). Approximately 500 ml of the water previously used to wash the beads was then poured carefully down the length of the trough, washing additional material into the funnel and down into the Nalgene bottle. The trough was scrubbed gently with a toothbrush, and the remaining ~500 ml of distilled water was used to rinse the trough completely. When this process was complete, the Nalgene bottle was capped, and the gasketed cap was replaced before repeating the process for the other four troughs. After this sequence, the clean collector was repositioned and levelled, and the glass beads were poured from the bags back into the troughs, leaving 5 L of water containing all the dust (Fig. 3).

Starting with the original collector deployments in 2011, the goal was to empty the collectors twice per year. A field visit as soon as possible after the snow had melted to provide access to the high elevations where the collectors were deployed, usually in July, yielded a sample of dust that had accumulated during the winter. A second visit as late as possible before the snow returned in the fall, usually October, yielded a sample of summer dust. This goal of biannual visits was achieved in some years, but because of weather, lingering snow, wildfire-related closures, and other complications it was not always possible to visit each collector that frequently. In addition, two collectors (DUST-2 and DUST-7) were also blown away by extreme winter winds at different times and needed to be replaced. Despite these challenges, the collector network yielded a total of 178 dust samples from 20 locations spanning 2011-2025.

3.2 Laboratory Methods

For each visit to a given dust collector, five 1-L bottles of dirty water were shipped back to the laboratory. Upon arrival, the bottles were organized on the counter and left to settle for several days, after which it was possible to pour approximately half of the water from each of the bottle, leaving the settled dust at the bottom. The remaining water and the dust were transferred to 50-ml centrifuge tubes that were spun at 6000 rpm in a 14-position rotor for 2 min to concentrate the dust. The supernatant water was decanted, and the dust was washed from the tube using a small spray bottle of distilled water. In this way, the dust from several 50-ml tubes was concentrated into a single tube, with the exact ratio depending on the amount of dust and remaining water. Through repetition of this process, it was eventually possible to concentrate all of the material from a given collector into a single 50-ml tube.

Material in each tube was then treated with 35% H_2O_2 for 5-10 days to remove disseminated organic matter fragments present in some samples. Reacting samples were contained with a fume hood and covered loosely with a layer of cellulose-based

https://doi.org/10.5194/essd-2026-423
Preprint. Discussion started: 13 July 2026

(Kimwipe) lab fabric. When the reaction slowed, ~10 ml of additional H_2O_2 was added (Aqua Solutions, technical grade), and care was taken to ensure that the samples did not dry out. When the reaction appeared to be over, tubes were transferred to an oven and held at a temperature of 60 °C for several hours. This final step stimulated a last burst of activity from the H_2O_2 which was necessary to ensure that the organic matter was completely consumed. After this point, the tubes were topped up to 45 ml with distilled water, centrifuged at 6000 rpm for 2 min, and the supernatant discarded again. This process was repeated to further wash the peroxide from the sample.

Next, the samples were wet sieved to 63 µm with distilled water. The material passing this sieve (clay and silt) was considered be exotic dust that was moved on for further analyses. In contrast, the sand-sized particles that failed to pass this mesh size were assumed to be sourced from the ground surface immediately surrounding the collector. Both size fractions were transferred into new, dry, 50-ml centrifuge tubes that had been pre-weighed.

The grain size distribution of the <63 µm fraction was then investigated with laser scattering using a Horiba LA-950. This instrument incorporates a red laser and blue light emitting diode (led), yielding an effective range from 10 nm to 3 mm. Both light sources were automatically aligned and blanked before each analysis, and the distilled water used to fill the flow cell was debubbled. A target transmittance of 80-90% for the red laser was used in guiding an automatic dilution process. If the autosampler delivered too little material to the instrument (laser transmittance >90%), then it returned to a given sample vial and transferred more to the instrument. On the other hand, if the red laser transmittance after injected the sample into the analyser was <80%, then the instrument automatically added distilled water, mixed, and dumped a random fraction of the sample, repeating as necessary until the transmittance was between 80 and 90%. Samples were physically stirred and sonified for 20 sec before each analysis, and a standard circulation and agitation speed of "5" was implemented (on a scale of 1, slowest, to 10, most energetic) as the injected sample was passed through the flow cell. Results were calculated from 10,000 acquisitions for both red and blue light to span the full grain size range, and to minimize the potential for rare outsized particles to skew the calculated size distribution. A refractive index of 1.54 with an imaginary component of 0.1i was used in the calculating the grain size distribution on a volume basis. Standard metrics including mean, median, mode, standard deviation, variance, and span were determined for each analysis. After each analysis, the instrument automatically filled and rinsed with distilled water three times to eliminate carryover to the next sample. The material used for grain size analysis was washed down the drain and not recovered, however the amount was very small compared with the total dust mass in a given sample.

After grain size analysis, the two size fractions (<63 µm and >63 µm) for each sample were dried overnight at 60 °C, and weighed again to determine the total mass of coarse (local) and fine (exotic) material in each collection from a given dust collector. The mass of the fine fraction (dust) was then combined with the duration of the collector deployment (days since it was last emptied) to calculate the depositional flux in $mg/m^2/day$.

https://doi.org/10.5194/essd-2026-423
Preprint. Discussion started: 13 July 2026

After massing, the coarse fraction was put aside and not analysed further. The fine fraction was emptied from the 50-ml centrifuge tube into a small agate mortar and pestle, and gently ground by hand to a powder. The colour of this powder was quantified using a Konica-Minolta CM-2600D colour spectrophotometer. The resulting colour was described in CIELAB nomenclature as three variables: L*, indicating darkness (0) to lightness (100); a*, indicating the balance of red (positive) and green (negative); and b*, indicating the balance of yellow (positive) to blue (negative). Spectral reflections were excluded (SCE format), and cumulative reflectance was also calculated in 10-nm bands from 360 to 740 nm. After colour quantification, the powdered dust sample was transferred to a small, labelled vial and reserved for future analyses.

Abundances of major and trace elements in the dust samples were determined by Inductively Coupled Plasma Optical Emission Spectrometry (ICP-OES) and Inductively Coupled Plasma Mass Spectrometry (ICP-MS) at different laboratories over the course of the project. Detection limits are listed in Table 2. Dust samples collected between 2011 and 2014, and 2017-2020 were analysed at SGS Minerals in Canada following digestion in HNO_3, HF, $HClO_4$, and HCl. Replicates were incorporated into each analysis run, along with standard OREAS-925. Samples collected in 2015 were analysed with an Agilent 8900 ICP-MS at Union College (New York, USA) following digestion in HF and HNO_3. Four USGS rock powder standards were used in each run: BIR-1 (basalt), NIST-688 (basalt), BHVO-2 (basalt), and NIST-278 (rhyolite). Five replicates were measured on each sample, and each sample was run in triplicate. Samples collected in 2016 and 2017 were analysed on a Thermo Fisher iCAP-Q ICP-MS at Middlebury College (Vermont, USA). Samples were dissolved in HNO_3 after fluxing with $LiBO_2$. A consistent set of four in-house standards was used for constructing a calibration curve, and each sample was run in triplicate. A quality-check (QC) sample was run after every five unknowns, and USGS standard RGM-1 (Rhyolite, Glass Mountain) was run after every 5 unknowns. Finally, samples collected in 2021-2024 were analysed on an Agilent 8900 ICP-MS at the University of Utah ICP-MS Metals and Strontium Isotope Facility. Samples following digestion in HNO_3 and HCl. The analysis runs included standard reference material 1643f (which was run in quadruplicate), multiple chemical blanks, and USGS standard AGV-1 (Andesite, Guano Valley, OR, USA).

https://doi.org/10.5194/essd-2026-423
Preprint. Discussion started: 13 July 2026

Open Access Earth System Science Data Discussions

Table 2: Detection Limits for Geochemical Analyses

Element	*2011-2014*	*2015*	*2016-2017*	*2017-2020*	*2020-21*	*2021-22*	2022-234
Lab	*SGS*	*Union*	*Midd*	*SGS*	*Utah*	*Utah*	*Utah*
Units	*mg/kg*	*mg/kg*	*mg/kg*	*mg/kg*	*mg/kg*	*mg/kg*	*mg/kg*
Al	1.0E-02	--	1.0E+02	1.0E-02	2.6E+02	6.7E+00	1.5E+00
As	1.0E+00	--	4.0E-01	5.0E+00	1.1E-01	4.9E-02	4.2E-02
Ba	1.0E+00	3.1E-02	4.0E-01	1.0E+01	1.0E+00	2.0E+00	4.3E-02
Be	1.0E-01	8.7E-03	4.0E-01	5.0E+00	7.8E-03	8.0E-03	1.3E-03
Bi	4.0E-02	--	4.0E-01	1.0E-01	1.6E-02	1.7E-03	--
Ca	1.0E-02	--	1.0E+02	1.0E-01	4.5E+01	8.3E+00	4.4E+00
Cd	2.0E-02	--	4.0E-01	2.0E-01	2.7E-02	3.6E-03	2.2E-03
Ce	5.0E-02	4.7E-01	4.0E-01	1.0E-01	2.0E-01	2.0E-01	7.3E-03
Co	1.0E-01	6.9E-03	4.0E-01	5.0E-01	2.6E-02	4.4E-03	3.1E-03
Cr	1.0E+00	5.5E-03	4.0E-01	1.0E+01	2.7E-02	1.4E-02	8.3E-01
Cs	5.0E+00	4.0E-04	4.0E-01	1.0E-01	--	--	1.7E-03
Cu	5.0E-01	9.4E-02	4.0E-01	1.0E+01	3.0E-01	1.9E-01	9.3E-02
Dy	5.0E-02	2.9E-03	4.0E-01	5.0E-02	8.6E-03	1.1E-02	5.7E-04
Er	5.0E-02	1.0E-03	4.0E-01	5.0E-02	5.0E-03	6.5E-03	4.2E-04
Eu	5.0E-02	5.9E-04	4.0E-01	5.0E-02	3.6E-03	3.1E-03	2.3E-04
Fe	1.0E-02	--	1.0E+02	1.0E-02	9.1E+01	1.7E+02	9.5E-01
Ga	1.0E-01	2.2E-02	4.0E-01	1.0E+00	3.0E-02	6.4E-02	7.0E-03
Gd	5.0E-02	5.9E-03	4.0E-01	5.0E-02	1.5E-02	1.2E-02	9.8E-04
Hf	2.0E-02	1.3E-03	4.0E-01	1.0E+00	1.8E-01	1.1E-01	1.9E-03
Ho	5.0E-02	3.3E-04	4.0E-01	5.0E-02	1.6E-03	2.2E-03	2.3E-04
K	1.0E-02	--	1.0E+02	2.0E-01	7.2E+01	4.8E+00	1.6E+02
La	1.0E-01	3.1E-03	4.0E-01	1.0E-01	1.5E-01	9.4E-02	4.6E-03
Li	1.0E+00	1.7E-02	4.0E-01	1.0E-01	--	--	8.8E-01
Lu	1.0E-02	3.5E-04	4.0E-01	1.0E+01	9.8E-04	9.1E-04	1.5E-04
Mg	1.0E-02	--	1.0E+02	5.0E-02	1.6E+01	2.0E+00	9.8E-01
Mn	2.0E+00	--	4.0E-01	1.0E-02	5.9E-01	2.3E-01	3.4E-02
Mo	5.0E-02	3.7E-03	4.0E-01	1.0E+01	9.0E-01	1.0E-01	3.2E-02
Na	1.0E-02	--	1.0E+02	2.0E+00	1.2E+01	3.0E+01	9.4E+01
Nb	1.0E-01	1.6E-03	4.0E-01	1.0E+00	2.0E-02	4.3E-02	1.6E-02
Nd	1.0E-01	6.2E-03	4.0E-01	1.0E-01	1.0E-01	7.9E-02	3.4E-03
Ni	5.0E-01	5.8E-02	4.0E-01	5.0E+00	2.1E-01	1.9E-02	4.5E-02
P	5.0E+01	--	4.0E-01	1.0E-02	2.1E+01	2.4E+01	9.4E-01
Pb	5.0E-01	8.0E-03	4.0E-01	5.0E+00	9.8E-02	2.5E-01	8.8E-03
Pb	--	--	4.0E-01	--	9.4E-02	2.3E-01	8.8E-03
Pb	--	--	4.0E-01	--	9.4E-02	2.4E-01	8.5E-03
Pr	5.0E-02	9.6E-04	4.0E-01	5.0E-02	2.8E-02	2.1E-02	9.7E-04
Rb	2.0E-01	5.6E-03	4.0E-01	2.0E-01	1.3E-02	8.3E-03	5.0E-02
Sb	5.0E-02	1.5E-01	4.0E-01	1.0E-01	8.1E-02	8.9E-02	1.7E-02
Sc	1.0E-01	--	4.0E-01	5.0E+00	7.7E-02	3.2E-02	8.5E-02
Se	2.0E+00	--	4.0E-01	--	--	--	2.0E-01
Sm	5.0E-02	1.4E-03	4.0E-01	1.0E-01	1.7E-02	1.5E-02	1.4E-03
Sn	3.0E-01	1.1E-02	4.0E-01	1.0E+00	1.7E-01	3.2E-03	3.4E-02
Sr	5.0E-01	1.1E-01	4.0E-01	1.0E+01	1.0E+00	1.9E-02	1.4E-02
Ta	5.0E-02	8.1E-04	4.0E-01	5.0E-01	6.0E-03	4.2E-03	1.8E-02
Tb	5.0E-02	2.9E-04	4.0E-01	5.0E-02	1.9E-03	1.8E-03	2.6E-04
Th	2.0E-01	7.1E-04	4.0E-01	1.0E-01	6.3E-02	3.5E-02	1.5E-02
Ti	1.0E-02	2.1E-04	4.0E-01	1.0E-02	2.3E+00	1.1E+01	2.2E-01
Tl	2.0E-02	--	4.0E-01	5.0E-01	1.6E-03	4.1E-03	7.1E-03
U	5.0E-02	4.4E-04	4.0E-01	5.0E-02	5.7E-03	1.0E-02	6.4E-04
V	2.0E+00	2.0E-02	4.0E-01	5.0E+00	4.8E-01	4.7E-02	1.5E-01
W	1.0E-01	--	4.0E-01	1.0E+00	5.3E-02	4.6E-02	5.4E-02
Y	1.0E-01	4.9E-03	4.0E-01	5.0E-01	6.0E-02	6.1E-02	2.9E-03
Yb	1.0E-01	1.7E-03	4.0E-01	1.0E-01	4.1E-03	6.5E-03	1.7E-04
Zn	1.0E+00	5.1E-01	4.0E-01	5.0E+00	2.5E+00	4.2E-01	4.9E-02
Zr	5.0E-01	1.1E-02	4.0E-01	5.0E-01	1.2E-01	5.9E-01	9.1E-02

https://doi.org/10.5194/essd-2026-423
Preprint. Discussion started: 13 July 2026

3.3 Data Compilation, Dissemination, and Sample Access

Each sample was registered in SESAR (System for Earth and Extraterrestrial Sample Registration) and assigned an IGSN (International Generic Sample Number). All IGSNs for samples generated as part of this project start with the prefix "IEMUN", identifying them as having been submitted by Jeffrey Munroe. Metadata for each include the location in which the sample was collected, the latitude and longitude coordinates of the sample site and its elevation, the associated dust collector, and the collection date.

Five datasets presenting the data resulting from the collector network were uploaded to the open EarthChem data repository following Creative Commons Attribution-ShareAlike 4.0 International, CC-BY-SA-4.0 (see Data Availability section). Each submission was assigned a DOI (Digital Object Identifier) and added to the EarthChem Library using a standard template. Metadata included as part of this template include information about the data source (investigator, contact information, related publications), the samples (their IGSNs, location where they were collected, the dust collector they represent, and the dates of the deployment), and information about the geochemical analyses (including instrumentation, dissolution procedures, detections limits, and blanks). Data included for each sample include their colour (L*, a*, b*), their grain size distribution (mean, median, and modal size, standard deviation, and percent abundance of standard grain size classes), and their geochemical characterization.

Material remaining after analysis was transferred to the Natural History Museum of Utah in Salt Lake City. Abstracts for each dataset in EarthChem were updated with the note "*Sample remaining after analysis is stored at the Natural History Museum of Utah in Salt Lake City. To access these samples for further analysis, please contact Mitchell Power (mitchell.power@geog.utah.edu) and with cc to Jeff Munroe (jmunroe@middlebury.edu).*" This archiving of the physical samples makes them accessible for future use by anyone who wants to analysis them as part of their future research.

4. Presentation and Overview of the Dataset

In total, the collectors comprising this network were visited 178 times between 2011 and 2024 (Fig. 4). Collector DUST-1 was emptied the greatest number of times (n=19). In contrast, DUST-19 and DUST-20, which were added near the end of the project, were emptied only once (Fig. 4).

https://doi.org/10.5194/essd-2026-423
Preprint. Discussion started: 13 July 2026

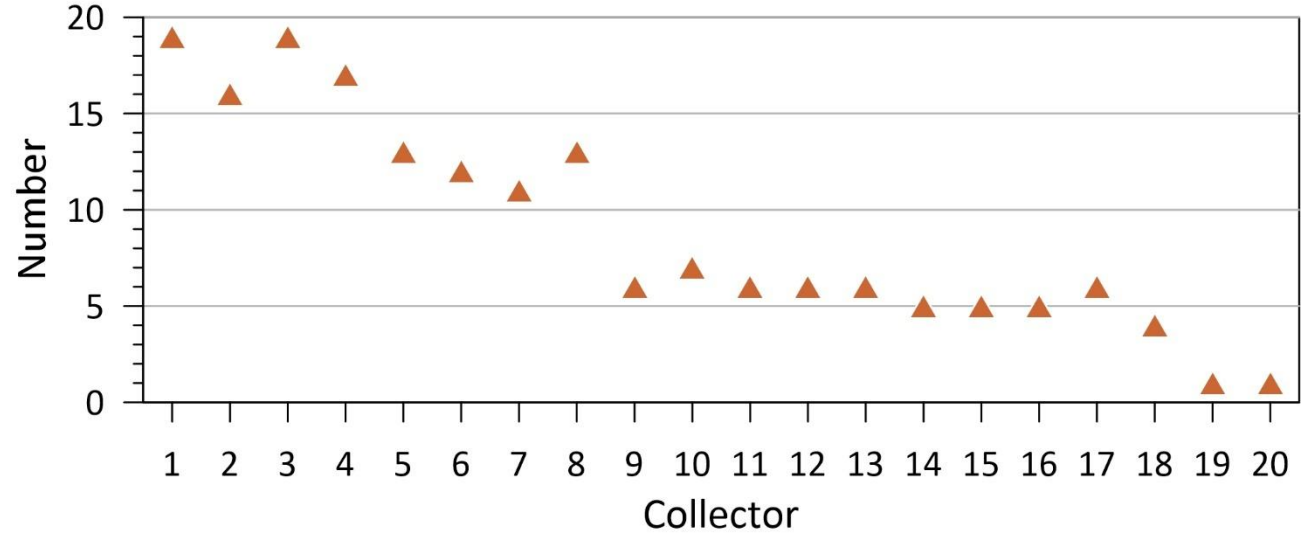

Figure 4. Collections at each of the 20 dust collectors between 2011 and 2024. The pattern generally follows the sequence in which the collectors were deployed (1-4 in 2011, 5-8 in 2015, 9-14 in 2020, 15-17 in 2021, and 18-20 in 2022). Finer scale differences reflect access issues (weather, snow, fire-related closures) that prohibited visits to specific collectors in certain years.

Durations (number of days) corresponding to each sample range from 62 to 839 days, with a mean of 271±172 days (Fig. 5). Sample masses ranged from 0.2 to 12.0 g, with a mean of 1.6±1.8 g. From these masses, durations, and the standard dimensions of the collectors, it was possible to calculate depositional fluxes (in mg/m^2/day) ranging from 1.9 to 353.9 with a mean of 25.9±41.6. This average is heavily influenced by a single collector (DUST-10, Fig. 2) where values were considerably higher than the other sites. The vast majority of samples represent depositional fluxes <20 mg/m^2/day (Fig. 5).

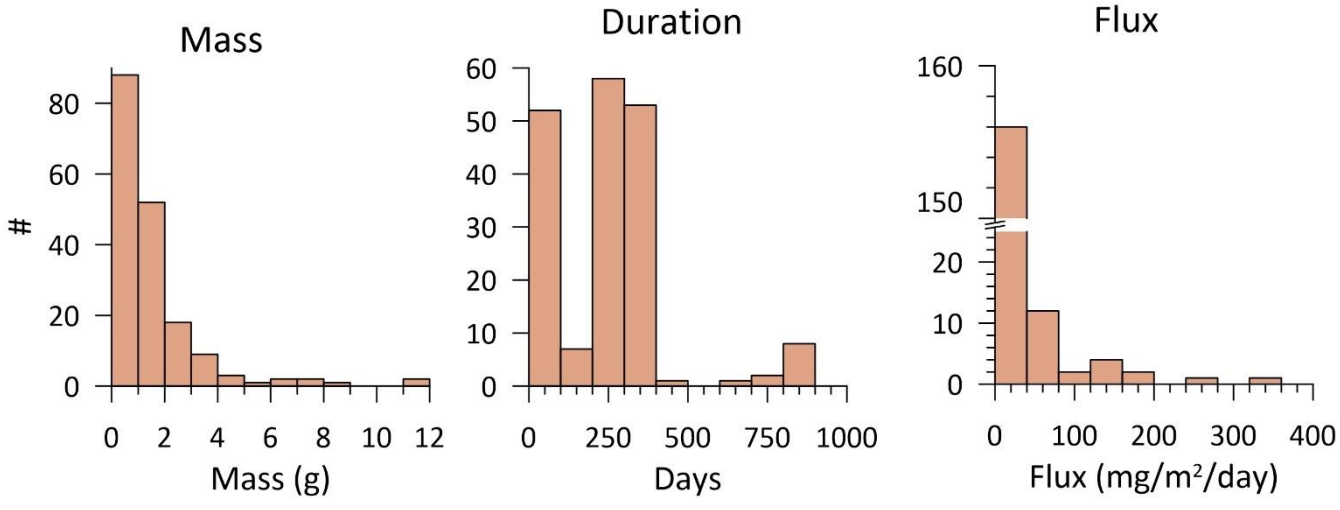

Figure 5. Distribution of sample masses (g), durations (days), and depositional fluxes (mg/m^2/day) across the entire dataset. Note that the Y-axis for the depositional flux histogram is logarithmic and broken from 25 to 150 to emphasize the distribution.

https://doi.org/10.5194/essd-2026-423
Preprint. Discussion started: 13 July 2026

Open Access Earth System Science Data Discussions

Colours (dry) were measured for 103 samples. Values of L* (darkness) range from 57.7 to 72.9 with a mean of 67.3±3.1 (Fig. 6), where a value of 0 corresponds to black, and 100 equals white. Values of a* range from 1.5 to 6.8 with a mean of 3.6±1.1 (Fig. 6). Positive values of a* indicate redness, with higher values corresponding to greater intensity. Values of b* range from 6.5 to 14.3 with a mean of 11.3±1.4 (Fig. 6). All b* values are positive, indicating that the dust has yellow hues. Overall, the average CIELAB colour designation for the dust (L* 67.3, a* 3.6, b* 11.3) corresponds to a light, desaturated yellowish beige colour, approximately equivalent to 8YR 6/2 in conventional Munsell designation.

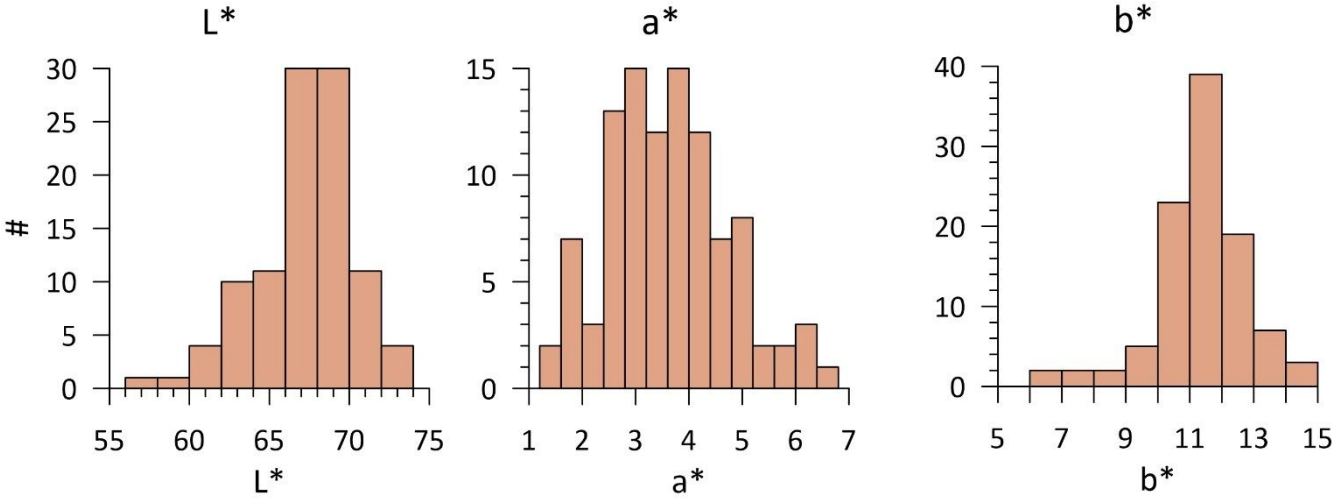

Figure 6. Histograms of colour variables measured in the dust sample, presented in CIELAB nomenclature. Values of L* indicate darkness, where 0 corresponds to black, and 100 equals white. Positive values of a* indicate redness, with higher values corresponding to greater intensity. Positive values of b* indicate that the dust has yellow hues.

Dust colours exhibit notable variability between sites, and between collections, with some consistencies (Fig. 7). The reddest dust is consistently collected at DUST-14 in the La Sal Mountains of southeastern Utah (Fig. 2). This location is downwind of extensive outcroppings of reddish Mesozoic sandstones. The darkest dust is typically collected at DUST-10 and DUST-17, which are the most urban of all the collector locations (DUST-10 was deployed on a roof in Salt Lake City, UT, and DUST-17 was located on a roof in Provo, UT). The lightest colour dust consistently comes from DUST-11 in the Ruby Mountains of Nevada (Fig. 2).

https://doi.org/10.5194/essd-2026-423
Preprint. Discussion started: 13 July 2026

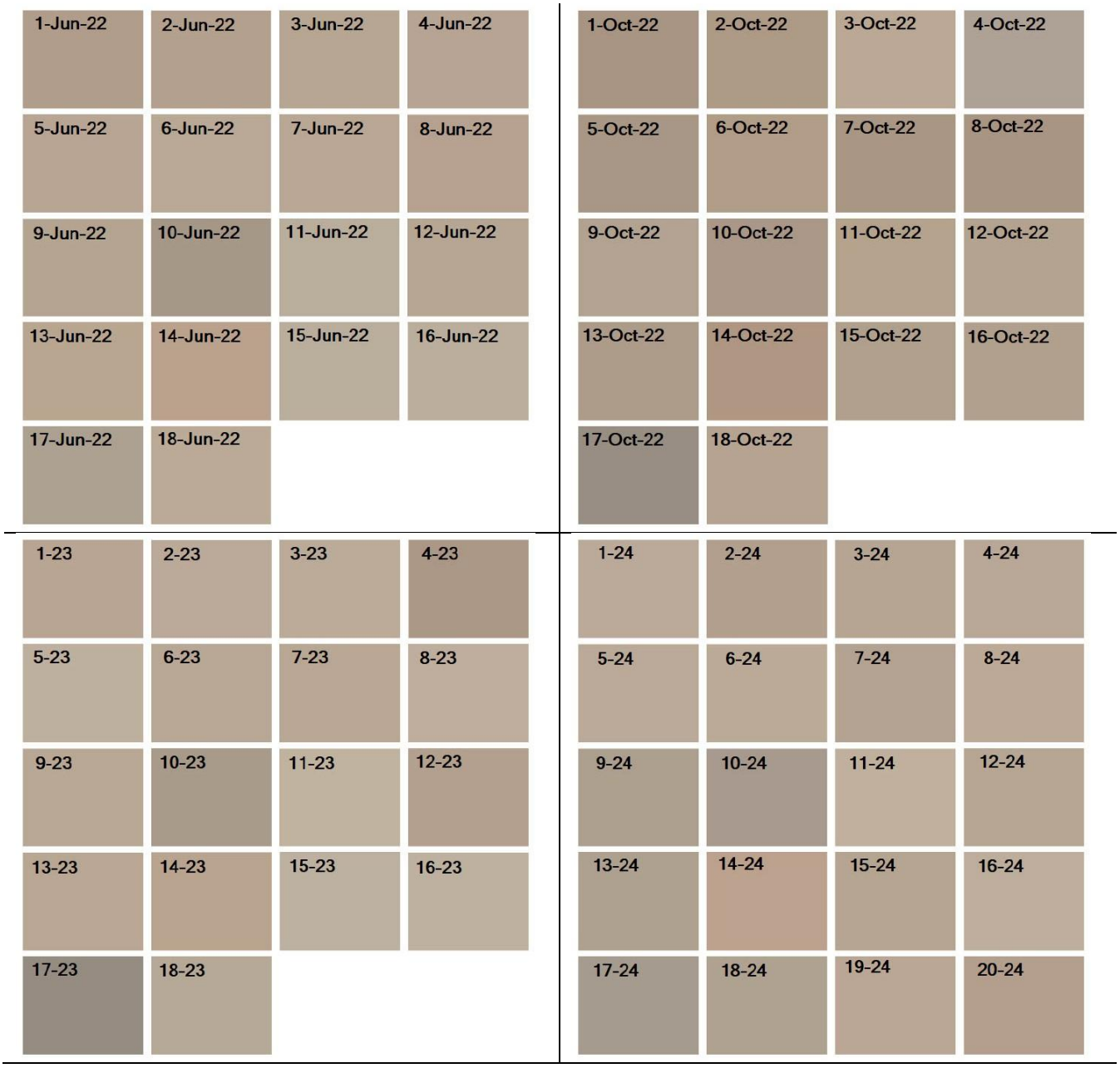

Figure 7. Colour blocks for dust samples showing within-year and inter-year variability. Upper left: winter dust from 2021-2022 (collected in June, 2022). Naming convention is Collector-Month-Year. Upper right: summer dust from 2022, collected in October, 2022. Naming convention is Collector-Month-Year. Lower left: annual dust from October, 2022 through October, 2023. Naming convention is Collector-Year. Lower right: annual dust from October, 2023 through October, 2024. Naming convention is Collector-Year.

https://doi.org/10.5194/essd-2026-423
Preprint. Discussion started: 13 July 2026

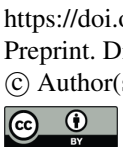

Open Access Earth System Science Data Discussions

The grain size distribution was investigated for all 178 samples. Mean grain sizes range from 8.1 to 26.2 µm, with an overall average of 15.6±3.2 µm (Fig. 8). Distribution means are generally greater than their corresponding median values for given samples, reflecting a positive skew toward infrequent, larger particles (Fig. 8). Accordingly, median grain sizes range from 5.9 to 19.8 µm (average of 10.7±2.5 µm). The most common particle size class in the dust samples is very fine silt (2-7 µm), which comprises 27% of the average sample (Fig. 8). Medium (14-30 µm) and fine (7-14 µm) silt are also >20% in most samples. In contrast, clay (<2 µm) is rare, as are particles with inferred diameters > 63 µm (sand).

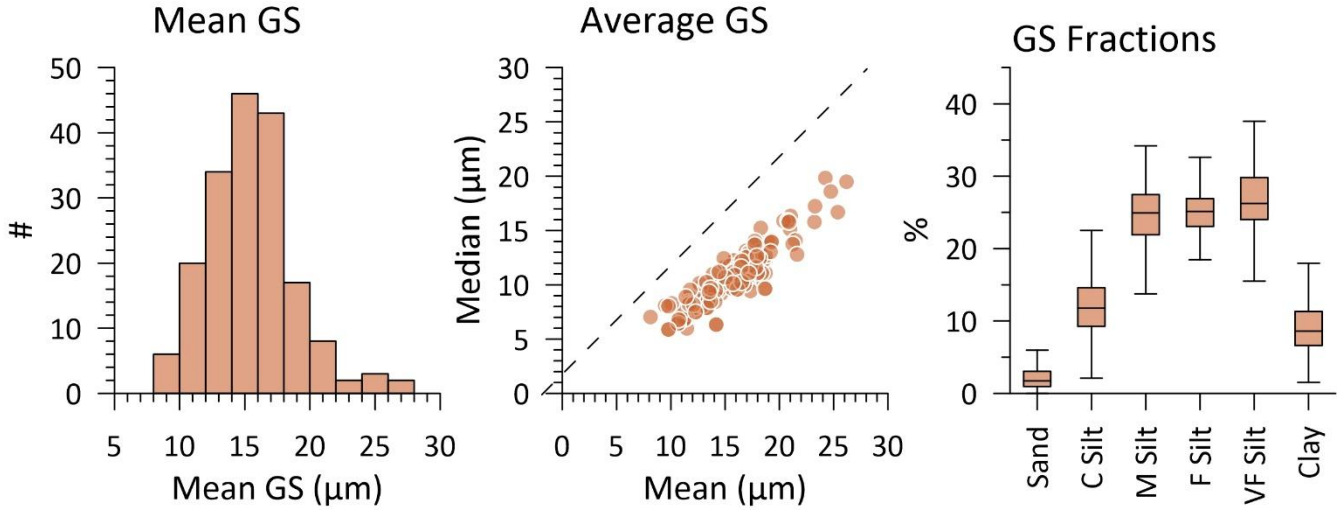

Figure 8. (Left) Histogram of mean grain sizes for dust samples. Most have means ~15 µm. (Middle) Biplot of mean and median grain size, illustrating that means are coarser than corresponding medians. Dashed line denotes the 1:1 relationship. (Right) Boxplot of grain size fractions in all the dust samples, showing that very fine silt (VF Silt) is the most common particle size class. Sand (>63 µm), Coarse Silt (C Silt, 30-63 µm), Medium Silt (M Silt, 14-30 µm), Fine Silt (F Silt, 7-14 µm), Very Fine Silt (VF Silt, 2-7 µm), and Clay (<2 µm).

Geochemical characterization was completed for 176 samples. Slightly different arrays of elements were measured at the different laboratories, however the abundance of a consistent suite of 44 elements was assessed in >95% of the samples (Al, As, Ba, Ca, Cd, Ce, Co, Cr, Cu, Dy, Er, Eu, Fe, Ga, Gd, Hf, Ho, K, La, Lu, Mg, Mn, Nb, Nd, Ni, Pb, Pr, Rb, Sb, Sc, Sm, Sn, Sr, Ta, Tb, Th, Ti, U, V, W, Y, Yb, Zn, Zr). Values below the detection limit (LOD) were replaced with LOD/2 in 19 instances (0.2% of the 8550 total measurements).

Major elements quantified in the samples, ranked in order of average abundance, are Al (7.1%) > Fe > K > Ca > Mg (1.1%) (Table 3, Fig. 9). The most abundant trace elements are Ti (4281±774 ppm), Ba (837±662 ppm) and Zn (551±814 ppm). Many elements are present at abundances exceeding their levels in average continental crust (Wedepohl, 1995) (Fig. 9). Eight

https://doi.org/10.5194/essd-2026-423
Preprint. Discussion started: 13 July 2026

Open Access Earth System Science Data Discussions

Table 3. Elements Quantified in Dust Samples, Ranked by Mean

Element	*Max mg/kg*	*Min mg/kg*	*Mean mg/kg*	*Stdev mg/kg*
Al	114190	28315	71425	12934
Fe	45403	16978	30010	4183
K	38188	82	23312	4130
Ca	69480	4802	15248	11593
Mg	24046	5728	11069	3484
Ti	9598	2300	4281	774
Ba	8809.7	415.3	836.7	662.19
Zn	6337.7	110.2	551.2	814.01
Mn	1562.0	168.8	502.9	244.56
Zr	681.9	37.0	212.2	68.24
Sr	375.6	83.1	196.2	43.51
Cu	1290.0	24.2	100.1	116.25
Rb	216.1	8.0	91.7	28.11
Pb	969.6	24.2	87.6	92.72
Ce	127.2	23.6	74.8	15.16
Cr	151.2	0.4	66.5	23.27
V	139.2	34.4	65.1	11.70
Sn	646.7	2.2	38.3	58.28
La	61.8	6.8	34.6	7.48
Ni	411.0	12.5	29.1	33.07
Nd	45.9	8.1	26.9	6.99
Y	43.7	1.4	22.7	4.77
Sb	117.2	0.7	17.9	25.11
Ga	28.4	9.7	17.8	2.94
Nb	33.1	3.0	15.4	3.76
Th	24.5	2.3	12.4	2.91
As	39.6	0.0	11.3	5.47
Co	31.5	4.5	9.8	2.86
Sc	12.6	0.0	8.8	1.53
Pr	12.3	2.1	7.7	1.42
Hf	17.3	2.2	5.6	1.67
Sm	8.2	1.6	5.5	0.93
Gd	7.5	1.3	4.8	0.83
Dy	7.4	1.2	4.4	0.74
U	7.3	1.5	3.8	0.80
W	20.6	0.0	3.0	2.02
Er	3.8	0.6	2.5	0.40
Yb	4.1	0.5	2.5	0.43
Cd	10.4	0.0	1.5	1.63
Eu	2.3	0.4	1.2	0.22
Ta	3.3	0.0	1.1	0.38
Ho	1.3	0.2	0.9	0.14
Tb	1.1	0.2	0.7	0.11
Lu	0.7	0.1	0.4	0.07

https://doi.org/10.5194/essd-2026-423
Preprint. Discussion started: 13 July 2026

elements have particularly high maximum and mean enrichment values: Sb (max 378x, mean 56x), Sn (max 257x, mean 15), Cd (max 102x, mean 14x), Zn (max 122x, mean 11x), Cu (max 90x, mean 7x), As (max 20x, mean 6x), Pb (max 57x, mean 5x), and W (max 15x, mean 2x). In contrast, the major elements Mg, K, and Ca have mean concentrations below their abundances in normal upper continental crust, as do some trace elements including Co, Ta, and Nb (Fig. 9).

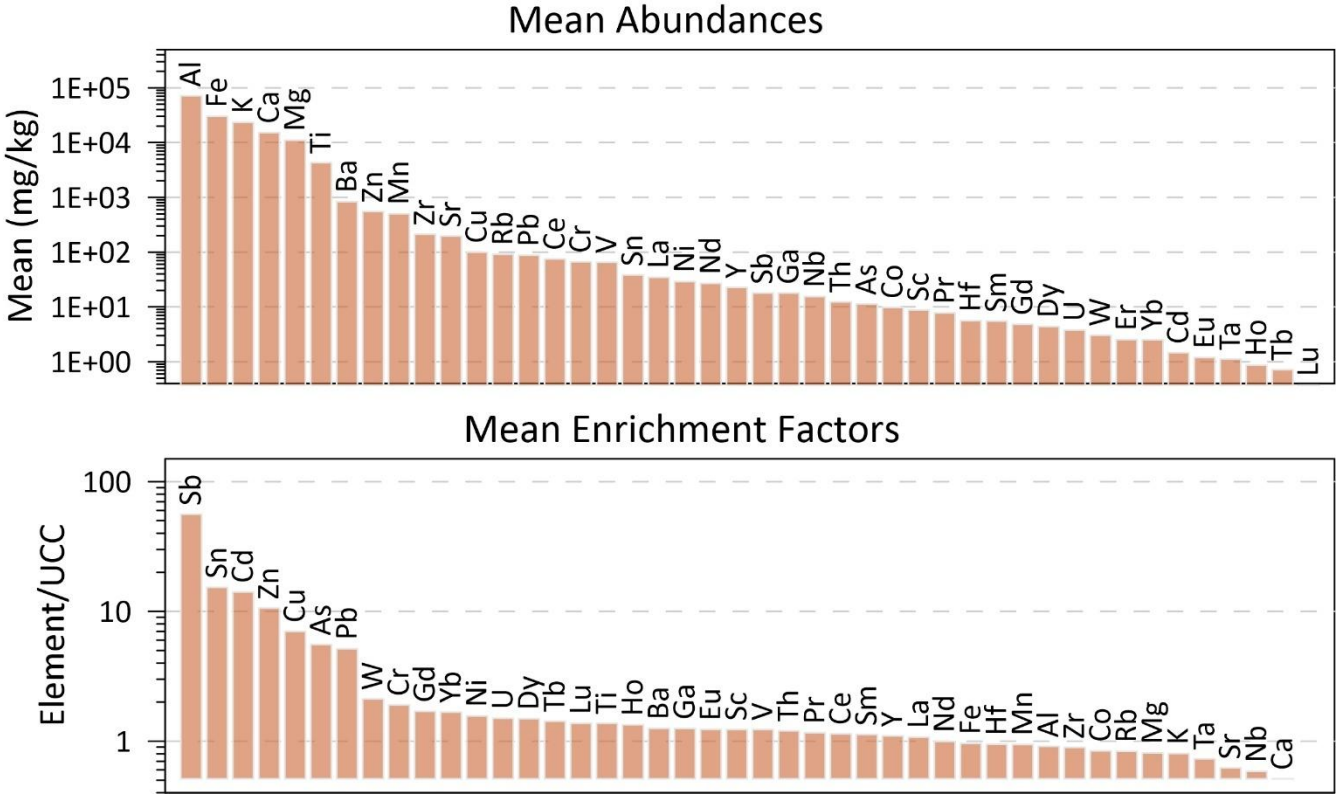

Figure 9. Geochemical summary of the dust samples. Top: Mean abundances (mg/kg) of the 44 elements quantified in at least 95 % of the dust samples. Bottom: Mean enrichment factors of these elements relative to their average abundance in upper continental crust (Wedepohl, 1995).

Notable differences become apparent when considering the distribution of values measured at each individual collector (Fig. 10). For instance, depositional flux (mg/m^2/day) is very high at DUST-10 (Salt Lake City), and very low at the two highest elevation collectors DUST-4 and DUST-12. Values of a* (redness) are consistently high at DUST-14, and low at DUST-17. Median grain size (µm) is greatest at DUST-10 and DUST-17, the two urban collectors. In contrast, collectors DUST-1 though DUST-8 in the Uinta Mountains have consistently finer median grain sizes (Fig. 10). Geochemistry also varies considerably through the collector network. For example, the ratio of immobile elements Ti/Zr averages ~20, but is highest at DUST-9, and lower at DUST-10, which is located not far away.

https://doi.org/10.5194/essd-2026-423
Preprint. Discussion started: 13 July 2026

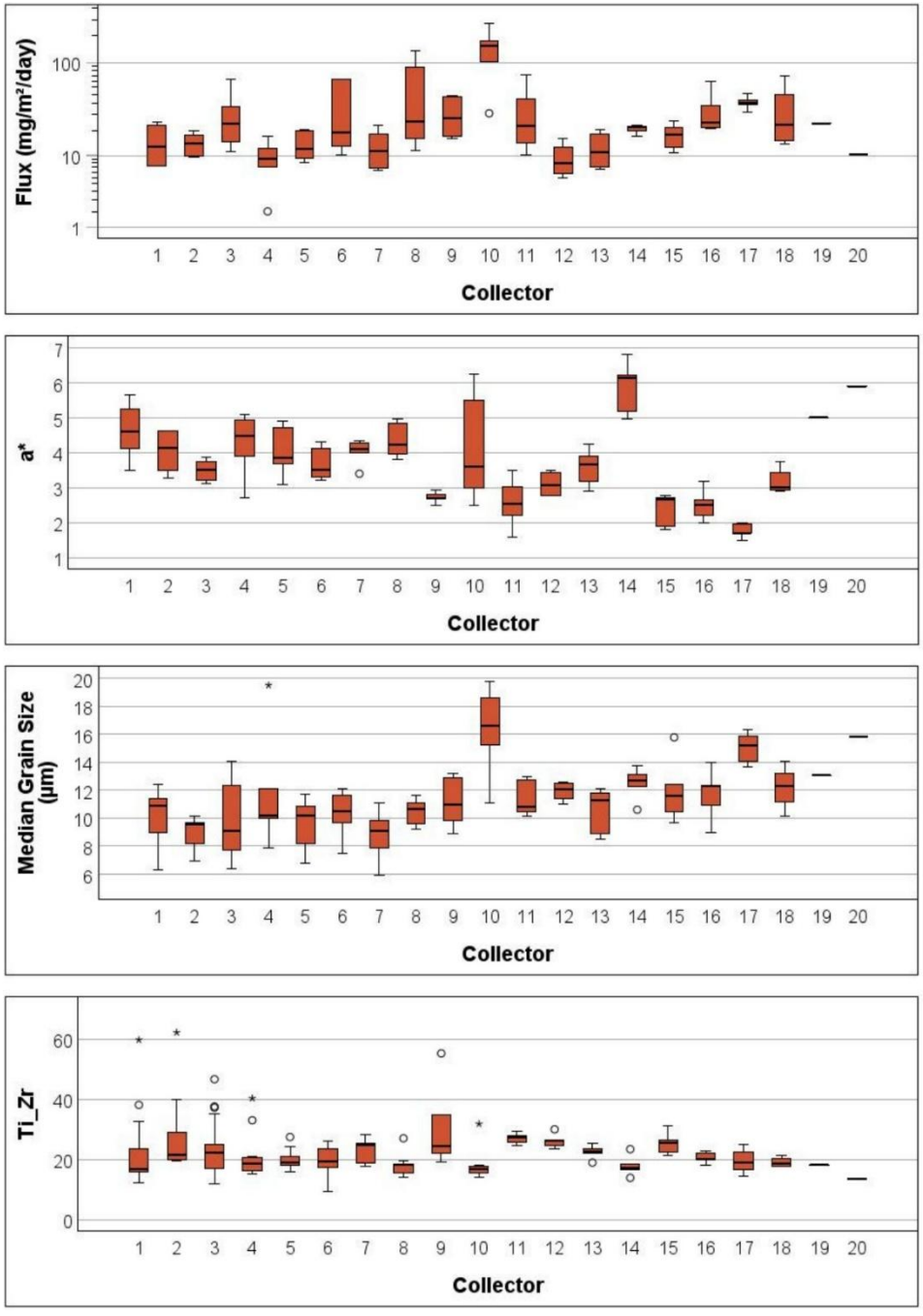

Figure 10. Boxplots of representative variables quantified for the dust samples presented as a function of dust collector. From top to bottom: depositional flux (in mg/m^2/day, note logarithmic scale), a* (redness), median grain size (µm), and the immobile element ratio Ti_Zr. In each plot, black line denotes the median, box spans the interquartile range (IQR), whiskers extend to 1.5-times the IQR, circles note outliers 1.5 to 3-times the IQR, and stars are extreme outliers more than 3-times the IQR.

https://doi.org/10.5194/essd-2026-423
Preprint. Discussion started: 13 July 2026

Open Access Earth System Science Data Discussions

Additional insight is revealed when considering the spatial variability in average values for the dust samples. For example, using the same metrics presented in Fig. 10, depositional flux of the dust is shown to be highest in the Salt Lake City urban area, intermediate in the Uinta Mountains, and relatively low in southern Utah (Fig. 11). Values of a* are high in southeastern Utah and in the Uinta Mountains, where bedrock with relatively red hues is widespread. Median grain size is high in the urban areas (DUST-10 and DUST-17), intermediate in Nevada and southern Utah, and relatively low in the Uinta Mountains. Values of Ti/Zr are much higher in Nevada than in Utah (with the exception of Salt Lake City), with some of the lowest values occurring in the Uinta Mountains (Fig. 11).

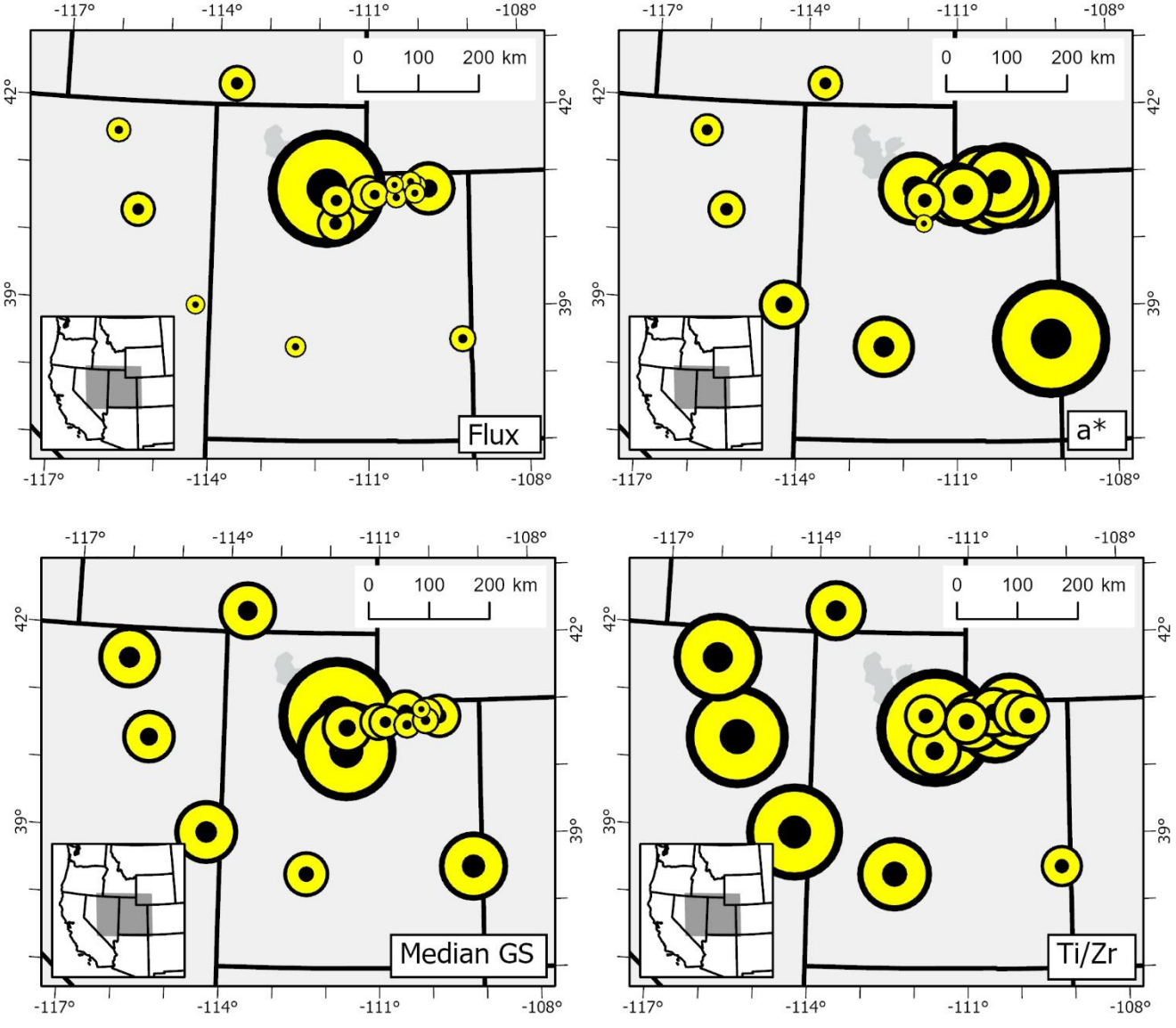

Figure 11. Spatial distribution of the metrics presented in Fig. 10. Upper left: depositional flux (in mg/m^2/day). Upper right: a* (redness). Lower left; median grain size (μm). Lower right: the immobile element ratio Ti/Zr. All symbols are proportional to mean values for individual collectors in the network (Fig. 2). The darker grey shape in the background is the outline of the Great Salt Lake. Inset shows location of the larger map (dark grey box) within the southwestern United States.

https://doi.org/10.5194/essd-2026-423
Preprint. Discussion started: 13 July 2026

Open Access Earth System Science Data Discussions

Data availability

The data discussed in this paper are presented in five files (Table 4) that are freely available in the EarthChem Library (Munroe, 2022a, 2023, 2024, 2026a, b).

Table 4. Datasets in the Open EarthChem Library Presenting Results from the Dust Sampler Network

Title	Year	URL
Data from the DUST^2 Project, Collectors DUST-1 through DUST-17, winter 2020-21 and summer 2021	2022	https://doi.org/10.26022/IEDA/112309
Dust Deposition in the Uinta Mountains, 2011-2021	2023	https://doi.org/10.26022/IEDA/112285
Data from the DUST^2 Project, Collectors DUST-1 through DUST-18, winter 2021-22 and summer 2022	2024	https://doi.org/10.26022/IEDA/113001
Data from the DUST^2 Project, collectors DUST-1 through DUST-18, Fall 2022 to Fall 2023	2025	https://doi.org/10.60520/IEDA/113846
Data from the DUST^2 Project, collectors DUST-1 through DUST-19, Fall 2023 to Fall 2024, and collectors DUST-19 through DUST-20, Fall 2022 to Fall 2024	2025	https://doi.org/10.60520/IEDA/113847

The title for each file clearly conveys both the time period covered by the data, and which dust collectors are represented. Each file is available in .csv format as a spreadsheet with five tabs. Tab 1: "Data Source" describes the dataset, lists the contact info for J. Munroe, and notes publications resulting from the data. Tab 2: "Samples" presents the sample name, IGSN, latitude/longitude/elevation of the collector, keywords identifying the location (mountain range), the number of the collector, the collection start and end dates, the collection duration (in days), the mass of dust collected and the corresponding depositional flux, the measured CIELAB colour parameters (L*, a*, b*), and information about the measured grain size distribution (mean, median, and modal size; standard deviation; total sand, coarse silt, medium silt, fine silt, very fine silt, total silt, and clay). Tab 3: "Data" repeats the sample name and IGSN, notes the analysed material was mineral dust in the <63 µm size fraction, describes the physical preparation of the samples and their chemical treatment, and notes the lab and analysis date. This information is followed by the abundances (in mg/kg) of elements quantified in the samples. Tab 4: "Primary Analytical Metadata" lists the elements quantified, the technique, the instrument used (if available), the laboratory, the analyst, and the analysis data. This information is followed by identification of a reference sample analysed, and the measured value of each element reported for the reference sample. Finally, Tab 5: "Method-specific Metadata" once again lists the elements quantified, their detection limit, and values for procedural blanks.

https://doi.org/10.5194/essd-2026-423
Preprint. Discussion started: 13 July 2026

Summary and Conclusions

This contribution presents a comprehensive dataset of geochemical measurements made on mineral dust samples collected between 2011 and 2025 as part of the DUST^2 Critical Zone Thematic Cluster and precursor projects. The data are freely available as a set of five files in the open EarthChem Library. The dataset integrates multi-year observations from a coordinated network of 20 passive dust collectors spanning a source-to-sink transect from arid and semi-arid dust-emitting regions of the Great Basin to downwind mountain environments in Utah, Nevada, and Idaho. For each sample, the dataset includes major and trace element concentrations, CIELAB colour determinations, and grain size metrics, together with metadata describing sampling locations, collection intervals, analytical procedures, and quality assurance protocols. By combining consistent sampling methods with standardized laboratory analyses across sites and years, this dataset provides a robust and internally comparable record of dust composition and variability across a well-constrained regional system.

A key contribution of this dataset is its ability to resolve both spatial and temporal variability in dust geochemistry across the source-to-sink continuum. The geographic distribution of sampling sites captures gradients in dust provenance and mixing, while repeated sampling at fixed locations enables evaluation of seasonal and interannual changes in composition associated with hydroclimatic variability and land-surface conditions. The inclusion of colour and grain size data provides a multi-dimensional framework for source attribution and for quantifying contributions from diverse dust-emitting regions. As such, the dataset is well suited for integration with atmospheric transport models, remote sensing products, and complementary environmental observations.

Beyond its regional focus, the dataset has broad relevance for Earth system science applications. It can be used to constrain dust source apportionment, to evaluate and improve model representations of dust emission and deposition, and to quantify the role of atmospheric inputs in soil formation, nutrient cycling, and water quality in downwind ecosystems. The dataset also provides a foundation for assessing how changes in climate, land use, and receding saline lakes may alter dust fluxes and composition in the future. Because similar processes operate in arid and semi-arid regions worldwide, this dataset offers a transferable framework for investigating dust-driven connectivity in other environmental settings.

In keeping with the goals of *Earth System Science Data*, all data and associated metadata are openly available in a standardized format to facilitate reuse. Detailed documentation of sampling design, analytical methods, and data processing ensures transparency and reproducibility, and supports integration with other datasets across disciplines. We anticipate that this dataset will serve as a resource for a wide range of users, including researchers studying aeolian processes, biogeochemical cycling, hydrology, and ecosystem dynamics, as well as those developing and validating Earth system models. By providing a consistent, multi-parameter record of dust composition across a coordinated monitoring network, this work contributes to improving data availability and interoperability for studies of mineral dust and its role in Earth's Critical Zone.

https://doi.org/10.5194/essd-2026-423
Preprint. Discussion started: 13 July 2026

Author contributions

JM: Conceptualization, Data curation, Formal analysis, Funding acquisition, Investigation, Methodology, Project administration, Validation, Visualization, Writing. DF: Formal analysis, Investigation, Writing.

Competing interests

The authors declare that they have no conflict of interest.

Acknowledgements

Thanks to E. Attwood, S. Lusk, R. McElroy, D. Munroe, E. Norris, S. O'Keefe, P. Olson, A. Proctor, A. Santis, E. Soderstrom, N. Stone, and L. Wasson for their assistance in the field and laboratory. T. Desautels and E. McMahon built the dust collectors at Middlebury College. Fieldwork for this project took place in the ancestral homelands of the Goshute, Shoshone, and Ute tribes.

Financial support

This work was supported by the US National Science Foundation awards EAR-1524476 and EAR-2012082 to J. Munroe.

https://doi.org/10.5194/essd-2026-423
Preprint. Discussion started: 13 July 2026

References Cited

Barnick, K. A., Green, A. M., Pendergast, M. E., and Şekercioğlu, Ç. H.: The effects of human development, environmental factors, and a major highway on mammalian community composition in the Wasatch Mountains of northern Utah, USA, Conservation Science and Practice, 4, e12708, https://doi.org/10.1111/csp2.12708, 2022.

Bockheim, J. and Koerner, D.: Pedogenesis in alpine ecosystems of the eastern Uinta Mountains, Utah, USA, Arct.Alp.Res., 29, 164–172, 1997.

Bockheim, J., Munroe, J., Douglass, D., and Koerner, D.: Soil development along an elevational gradient in the southeastern Uinta Mountains, Utah, USA, Catena, 39, 169–185, 2000.

Brahney, J., Heindel, R. C., Gill, T. E., Carling, G., Gonzalez-Olalla, J. M., Hand, J., Mallia, D. V., Munroe, J. S., Perry, K., and Putman, A. L.: Dust in the Critical Zone: North American case studies, Earth-Science Reviews, 258, 104942, 2024.

Checketts, H. N., Carling, G. T., Fernandez, D. P., Nelson, S. T., Rey, K. A., Tingey, D. G., Hale, C. A., Packer, B. N., Cordner, C. P., and Dastrup, D. B.: Trace Element Export From the Critical Zone Triggered by Snowmelt Runoff in a Montane Watershed, Provo River, Utah, USA, Frontiers in Water, 2, 2020.

Formenti, P., Schütz, L., Balkanski, Y., Desboeufs, K., Ebert, M., Kandler, K., Petzold, A., Scheuvens, D., Weinbruch, S., and Zhang, D.: Recent progress in understanding physical and chemical properties of African and Asian mineral dust, Atmospheric Chemistry and Physics, 11, 8231–8256, 2011.

Formenti, P., Caquineau, S., Desboeufs, K., Klaver, A., Chevaillier, S., Journet, E., and Rajot, J.-L.: Mapping the physico-chemical properties of mineral dust in western Africa: mineralogical composition, Atmospheric Chemistry and Physics, 14, 10663–10686, 2014.

Lang, O. I., Meyer, J., Hu, J. M., and McKenzie Skiles, S.: Darkened Snow Triggers Different Snowmelt Responses Over Contrasting Water Years in Great Salt Lake Headwater Basins, Water Resources Research, 62, e2025WR041598, https://doi.org/10.1029/2025WR041598, 2026.

Munroe, J. S.: Properties of modern dust accumulating in the Uinta Mountains, Utah, USA, and implications for the regional dust system of the Rocky Mountains, Earth Surf.Process.Landforms, 39, 1979–1988, 2014.

Munroe, J. S.: Data from the DUST^2 Project, Collectors DUST-1 through DUST-17, winter 2020-21 and summer 2021, EarthChem [dataset], https://doi.org/doi.org/10.26022/IEDA/112309, 2022a.

Munroe, J. S.: Relation between regional drought and mountain dust deposition revealed by a 10-year record from an alpine critical zone, Science of The Total Environment, 844, 156999, 2022b.

Munroe, J. S.: Dust Deposition in the Uinta Mountains, 2011-2021, EarthChem [dataset], https://doi.org/https://doi.org/10.26022/IEDA/112285, 2023.

Munroe, J. S.: Data from the DUST^2 Project, Collectors DUST-1 through DUST-18, winter 2021-22 and summer 2022, EarthChem [dataset], https://doi.org/doi.org/10.26022/IEDA/113001, 2024.

Munroe, J. S.: Data from the DUST^2 Project, collectors DUST-1 through DUST-18, Fall 2022 to Fall 2023, EarthChem [dataset], https://doi.org/doi.org/10.60520/IEDA/113846, 2026b.

https://doi.org/10.5194/essd-2026-423
Preprint. Discussion started: 13 July 2026

Munroe, J. S.: Data from the DUST^2 Project, collectors DUST-1 through DUST-19, Fall 2023 to Fall 2024, and collectors DUST-19 through DUST-20, Fall 2022 to Fall 2024, EarthChem [dataset], https://doi.org/doi.org/10.60520/IEDA/113847, 2026a.

Munroe, J. S.: Mineral dust and the global critical zone, Earth Critical Zone, 3, 100052, https://doi.org/10.1016/j.ecz.2025.100052, 2026c.

Munroe, J. S., Attwood, E. C., O'Keefe, S. S., and Quackenbush, P. J.: Eolian deposition in the alpine zone of the Uinta Mountains, Utah, USA, Catena, 124, 119–129, 2015.

Munroe, J. S., Norris, E. D., Carling, G. T., Beard, B. L., Satkoski, A. M., and Liu, L.: Isotope fingerprinting reveals western North American sources of modern dust in the Uinta Mountains, Utah, USA, Aeolian Research, 38, 39–47, 2019.

Munroe, J. S., Norris, E. D., Olson, P. M., Ryan, P. C., Tappa, M. J., and Beard, B. L.: Quantifying the contribution of dust to alpine soils in the periglacial zone of the Uinta Mountains, Utah, USA, Geoderma, 378, 114631, 2020.

Munroe, J. S., McElroy, R., O'Keefe, S., Peters, A., and Wasson, L.: Holocene records of eolian dust deposition from high-elevation lakes in the Uinta Mountains, Utah, USA, Journal of Quaternary Science, 36, 66–75, 2021.

Munroe, J. S., Soderstrom, E. J., Kluetmeier, C. L., Tappa, M. J., Mallia, D. V., and Bauer, A. M.: Regional sources control dust in the mountain critical zone of the Great Basin and Rocky Mountains, USA, Environ. Res. Lett., 18, 104034, https://doi.org/10.1088/1748-9326/acfb26, 2023.

Munroe, J. S., Santis, A. A., Soderstrom, E. J., Tappa, M. J., and Bauer, A. M.: Mineral dust and pedogenesis in the alpine critical zone, SOIL, 10, 167–187, https://doi.org/10.5194/soil-10-167-2024, 2024.

Munroe, J. S., Carling, G. T., Perry, K. D., Fernandez, D. P., and Mallia, D. V.: Mixing of natural and urban dust along the Wasatch Front of northern Utah, USA, Sci Rep, 15, 3851, https://doi.org/10.1038/s41598-025-88529-9, 2025.

Nielson, J. R. and Brahney, J.: Quantifying Dust Nutrient Mobility Through an Alpine Watershed, JGR Biogeosciences, 130, https://doi.org/10.1029/2024jg008175, 2025.

Rodríguez, S., Alastuey, A., Alonso-Pérez, S., Querol, X., Cuevas, E., Abreu-Afonso, J., Viana, M., Pérez, N., Pandolfi, M., and De La Rosa, J.: Transport of desert dust mixed with North African industrial pollutants in the subtropical Saharan Air Layer, Atmospheric Chemistry and Physics, 11, 6663–6685, 2011.

Shao, Y., Wyrwoll, K.-H., Chappell, A., Huang, J., Lin, Z., McTainsh, G. H., Mikami, M., Tanaka, T. Y., Wang, X., and Yoon, S.: Dust cycle: An emerging core theme in Earth system science, Aeolian Research, 2, 181–204, 2011.

Wedepohl, K. H.: The composition of the continental crust, Geochim.Cosmochim.Acta, 59, 1217–1232, 1995.